

NON-EVAPORABLE GETTER-BASED DIFFERENTIAL PUMPING SYSTEM FOR SRILAC AT RIBF

H. Imao, K. Yamada, N. Sakamoto, T. Watanabe, Y. Watanabe, O. Kamigaito
RIKEN Nishina Center for Accelerator-based Science, Saitama, Japan
K. Oyamada
Sumitomo Heavy Industries Accelerator Science Ltd., Tokyo, Japan

Abstract

Upgrades of the RIKEN heavy-ion linac (RILAC) involving a new superconducting linac (SRILAC) are undergoing to promote super-heavy element searches at the RIKEN Radioactive Isotope Beam Factory (RIBF). Stable ultra-high vacuum ($<10^{-8}$ Pa) and particulate-free conditions are strictly necessary for keeping the performance of the super-conductive radio frequency (SRF) cavities of the SRILAC. It is crucially important to develop neighboring warm sections to prevent contamination from the existing old RILAC and beamlines built almost four decades ago.

In the present study, non-evaporable getter-based differential pumping systems were newly developed to achieve the pressure reduction from the existing beamline vacuum (10^{-5} – 10^{-6} Pa) to the ultra-high vacuum within very limited length (<80 cm) ensuring the large beam aperture of more than 40 mm. They are also equipped with compact electrostatic particle suppressors.

INTRODUCTION

Upgrades of the RIKEN heavy-ion linac (RILAC) [1] involving a new superconducting linac (SRILAC) [2-6] and a new 28-GHz superconducting electron-cyclotron-resonance ion source [7] are undergoing. The aim, as a first priority, of the upgrades is to promote super-heavy element searches [8] at the RIKEN Radioactive Isotope Beam Factory (RIBF) [9].

The SRILAC consists of three cryomodules (CM1, CM2, CM3). The CM1 and CM2 have four quarter-wavelength resonators (QWRs), the superconducting radio frequency (SRF) accelerator cavities, respectively. The CM3 have two QWRs. The resonant frequency of the QWRs is 73 MHz optimized for $\beta = 0.078$ and the target Q value is $1 \cdot 10^9$ with an accelerating gradient of 6.8 MV/m. The three cryomodules, CM1-3, will be installed into the existing beamline between the RILAC, remaining 8 drift tube linac (DTL) tanks (#1–#6, A1, A2) in the new configuration, and the high energy transport (HEBT) as shown in Fig. 1.

A stable ultra-high vacuum (UHV) condition ($<10^{-8}$ Pa) and an almost particle-free condition are necessary not only in the SRF cavities but also in the neighboring warm sections to prevent contaminations of the SRF cavities, which cause various unwanted problems, e.g., Q-decrease and field emissions, in long-term operations. Unfortunately, the vacuum pressures of the RILAC and the existing beamlines, built almost four decades ago, are not so good (10^{-5} – 10^{-6} Pa). The wall surfaces at the inside of the ducts and chambers in the beamlines are dirty due to the long-time accelera-

tor operation with beam-destructive diagnostics and fragile carbon-foil strippers. To install the SRF system into such an old existing normal conducting (NC) accelerator demands special cares and an important challenging issue itself.

In the present study, non-evaporable getter (NEG)-based differential pumping system (DPS) has been developed. The pair DPSs will be placed upstream and downstream of the SRILAC, respectively, to mitigate the large difference of the vacuum and the clean conditions.

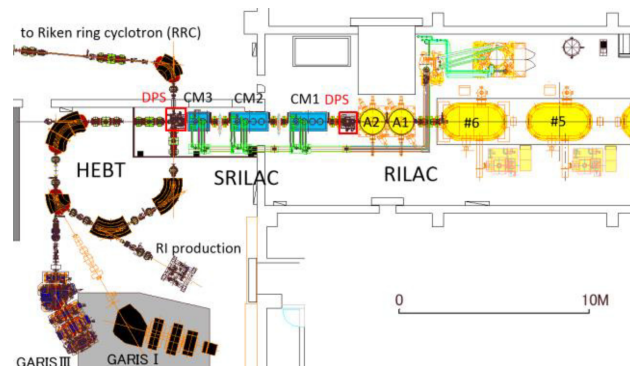


Figure 1: The CM1-3 are installed between the RILAC and the HEBT. The pair DPSs are placed upstream and downstream of the SRILAC. There are two active experimental lines connected to the HEBT, for GARIS III and RI productions.

DESIGN AND ASSEMBLING

The present system is the three-stage DPS as shown in Fig. 2. It was designed to achieve the pressure reduction from the existing beamline vacuum (10^{-5} – 10^{-6} Pa) to the ultra-high vacuum less than 10^{-8} Pa of the SRF cavities within very limited length only 75 cm ensuring beam aperture more than 40 mm. The properties of pumps we used for the DPS are summarized in the bottom of Fig. 2. The first stage is the preparation stage to connect to the NEG-based vacuum. We use a turbo-molecular pump (HiPace700; Pfeiffer vacuum GmbH) with a dry roughing pump (NeoDry60E; Kashiyama Industries, Ltd.) and a cryogenic pump (CRYO-U6H; ULVAC, Inc.) at the first stage to evacuate most of gas species including N₂, H₂O, H₂ and He with first pumping speeds. The performance of the pumping at the first stage is important to extend the reactivation cycle of the NEG pumps in the subsequent stages.

At the second stage, a high-vacuum NEG pump of ZAO® alloy (Capacitorr HV1600; SAES Getters S.p.A.) and an

ion pump (Vacon Plus 200 (VP200); Agilent Technologies, Inc.) are equipped. The HV1600, which is the main pump of the system, have high pumping speed for hydrogen (1400 L/s in nominal value) and large absorption capabilities suitable for the working pressure at 10^{-7} – 10^{-8} Pa. The VP200 is important to pump out the small fraction of inert gas and CH₄ because the NEG pumps have almost no pumping power to them.

The latest-released UHV NEG pumps of ZAO® alloy (Capacitor Z400; SAES Getters S.p.A.), which can provide ultra-high vacuum compatible to the SRF cavities [10], are equipped at the third stage.

Optimizations of the system design were performed with the Molflow+ which is a Monte-Carlo simulation code developed at CERN [11]. The expected time interval for the reactivation of the NEG pumps in the present design are more than 1 year which is sufficient for our operations.

The DPS should have the protection system from unexpected vacuum breaks. There are two active experimental lines connected to the HEBT, one is the line for radioactive-isotope production, and the other is the line for gasfilled recoil ion separator (GARIS III), searching for super heavy elements. Both experiments have potential risk of gas rushing to the vacuum. The DPS have a fast closing gate valve (Series 75.2; VAT Group AG) responses within 10 ms after receiving the signal of the pressure rise of distributed three cold-cathode gauges.

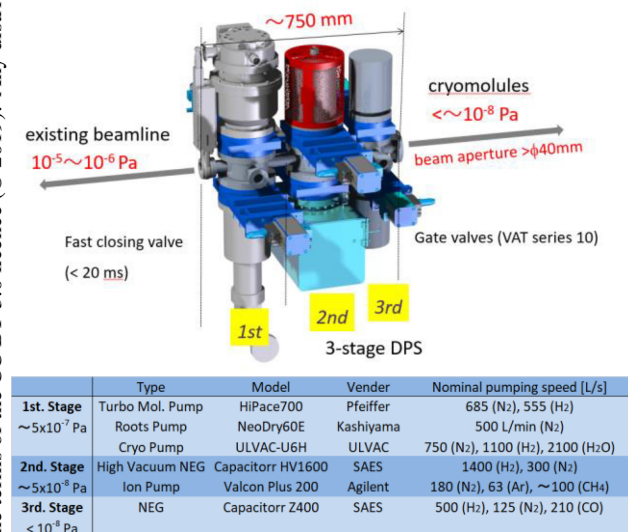


Figure 2: Design view of the three-stages DPS and basic properties of pumps we used.

All components (chambers, pumps, valves, vacuum gauges, etc.) are cleaned and assembled in a clean room ISO class 1 (Fig. 3). Preliminary surface treatments of the vacuum chambers are performed in the professional company (SAN AI PLANT Co., Ltd.); alkaline cleaning, acid cleaning, ultra-pure water cleaning, passivation treatment and blowing with dry air. We further performed high-pressure rinsing with 8-MPa ultra-pure water, vacuum baking at 120°C for 24 hours and blowing with an ionizing gas gun

(TG-3; Simco Company, Inc.) monitoring the emission of particles by a particle counter (HHPC6+; Beckman Coulter, Inc.) in the ISO-1 clean room. All pumps, gauges (TPR018 Pirani gauge and IKR070 cold-cathode gauge; Pfeiffer vacuum GmbH) and UHV gate valves (Series 10; VAT Group AG) are also blown carefully with the ionizing gas gun.

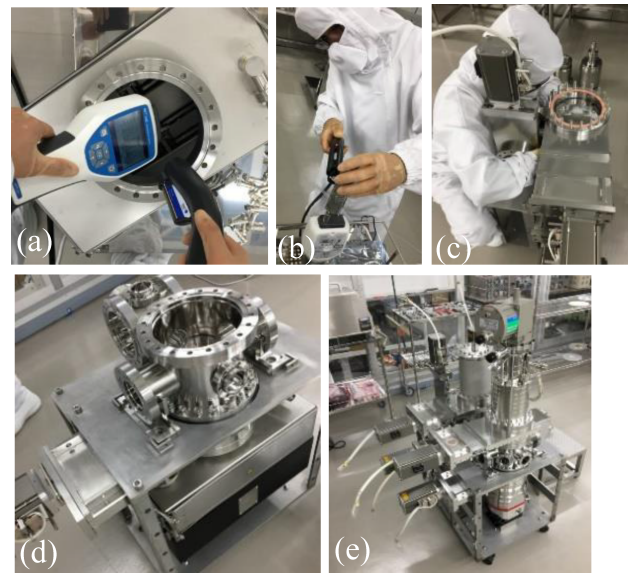


Figure 3: Cleaning and assembling of the DPS in the ISO-1 clean room; blowing of the VP200 with the ionizing gun (a), blowing of the Z400 (b), assembling the gate valve (c), vacuum chamber for the NEG pumps (d), assembled DPS for performance tests (e).

Figure 4 shows the results of particle count tests for Z400s before and after the reactivation performed in ISO class 6 environment. Particle counts after the activation are significantly reduced.

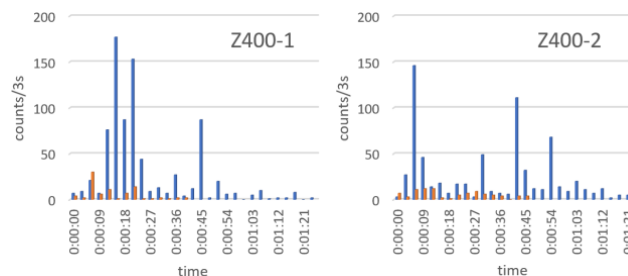


Figure 4: Particle counts ($>0.3 \mu\text{m}$) during the blowing with the ionizing gun for two Z400s before (blue bars) and after (red bars) the reactivation process.

PERFORMANCE TESTS

We performed the performance tests of the DPS in a clean room ISO class 6 (Fig. 5). The DPS was pumped out and baked at 120°C for five days before the tests. The pressure reached to approximately 2×10^{-9} Pa after the baking. After that, we measured the pressures of three stages in the DPS when we leaked N₂, H₂, and He from the beamline side.

The flow amount of the leaked gas was controlled with a variable leak valve. The observed pressures shown in Fig. 5 are in good agreement with the calculated ones with the Molflow+ for all gas species. We used nominal pumping speeds for all pumps and degassing from the chamber's wall was disregarded in the calculations. We demonstrated successfully the pressure reduction from 10^{-5} – 10^{-8} Pa for N₂ and H₂ in 75 cm with the beam aperture of more than 40 mm.

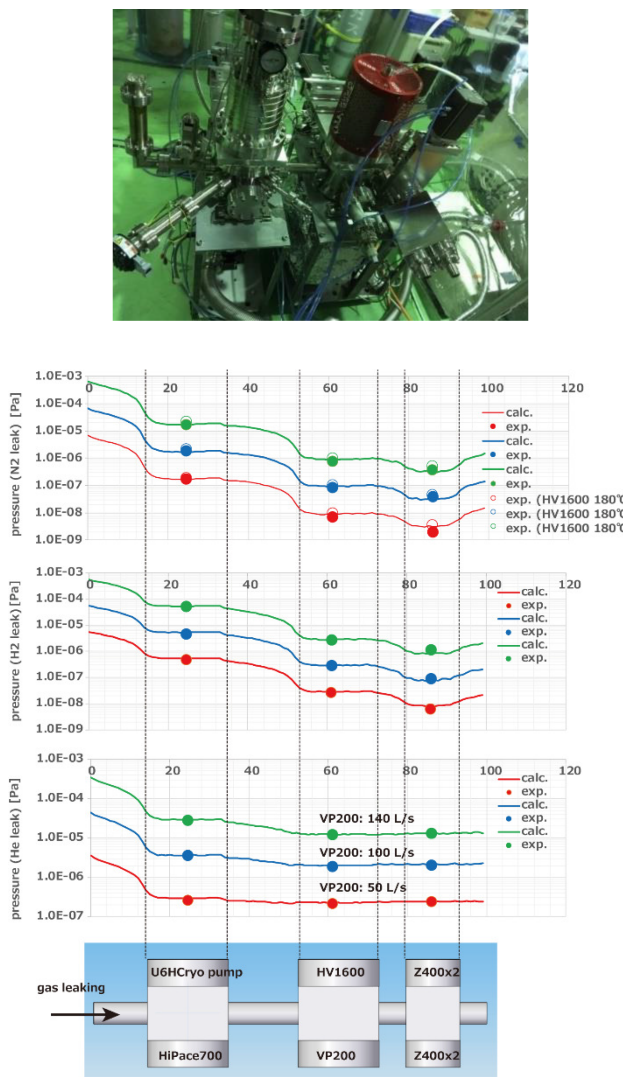


Figure 5: A picture of the DPS during the performance tests (upper) and the measured and calculated pressure distributions in the DPS for N₂, H₂ and He leaking (bottom).

ELECTROSTATIC PARTICLE SUPPRESSOR

A compact electrostatic particle suppressor (EPS) has been developed to suppress the scattering of particles and reduce possibilities to transport particles to the SRF cavities. The EPS will be equipped at the inside of the firststage chamber of the DPS.

SRF Technology - Ancillaries
vacuum

The EPS consists of two electrodes, each of them consists of 6 stainless steel bars as shown in Fig. 6. We can apply high voltage up to ± 10 kV on both electrodes of the EPS. The electrodes are optimized with a FEA software Opera 3D (Dassault Systems GmbH). The trajectory of the beams (e.g., $^{51}\text{V}^{13+}$ beams with the energy of 6.5 MeV/u) and particles (stainless steel with the diameter of 0.2 μm) when high voltage of ± 6 kV are applied on the electrodes were calculated as shown in Fig. 6. The deflection angle of $^{51}\text{V}^{13+}$ beams due to the electric field is less than 0.5 mrad, which is easily recoverable in the following steering magnets.

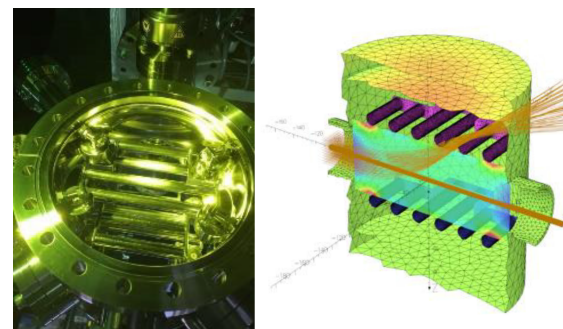


Figure 6: A picture of the electrostatic particle suppressor and calculated trajectory for the stainless steel particles ($\phi 0.2 \mu\text{m}$) with a single charge state and $^{51}\text{V}^{13+}$ beams.

Some particle tests with the EPS in the air and vacuum were performed with a vacuum particle sensor (Wexx co., Ltd). Figure 7 shows the dependence of the particle counts on the applied voltage after fast venting. The vacuum chamber was vented with air at the outside of the clean room in the test. The particles (> 0.3 mm) were counted with the particle counter. The half-life of the flying particles is approximately 1 hour in natural condition. The lifetime of the flying particles is reduced drastically when we applied +6 kV on an electrode of the EPS.

Figure 8 shows the particle counts of tungsten particles artificially generated above the electrodes. A tense tungsten wire was scraped by using a hand grinder with ceramic drill bit in the air. The same kind of tests were performed in vacuum. Figure 9 shows particle counts of ceramic particles artificially generated by scraping a ceramic block in vacuum. Particle counts were significantly reduced when we applied high voltage on the electrodes in both particle tests. The vacuum in the beamlines become an ionizing environment due to the energetic heavyion passing during the operation. We expect the EPS can suppress the particle transport to the SRF cavities in such an environment.

CLEANING OF BEAMLINE

The wall surfaces in the vacuum ducts, diagnostic chambers and bending magnet chambers in the HEBT are quite dirty due to the long-time operations. Figure 10 shows the picture of the inside of the chambers inspected with a fiber scope. There are many visible dusts as shown in Fig. 10. The dusts were sampled and analysed by using an electron

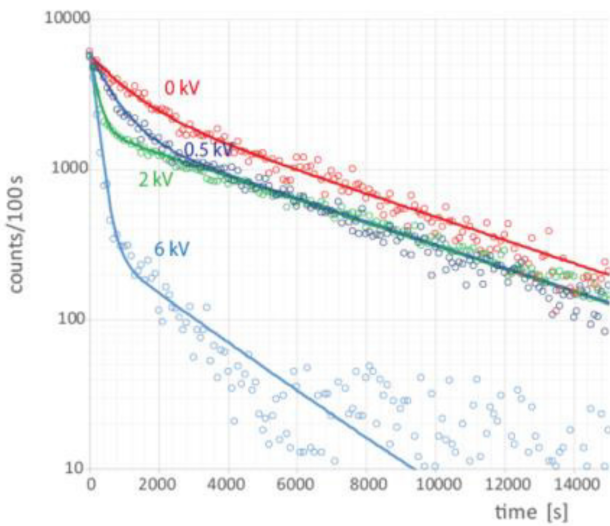


Figure 7: Dependence of particle counts ($> 0.3 \mu\text{m}$) after the fast venting on the applied voltage on the EPS. Solid lines indicate fitted lines using two exponentials.

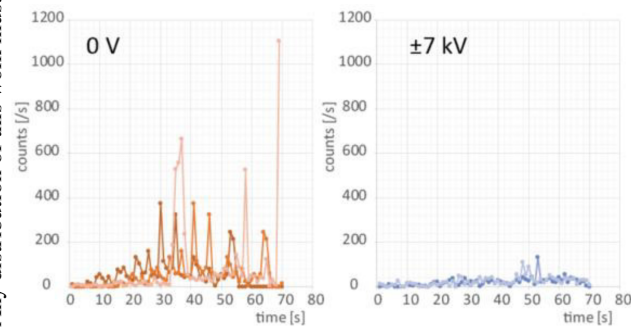


Figure 8: Particle counts ($> 0.3 \mu\text{m}$) when a tungsten wire was scraped by using a hand grinder with a ceramic drill bit with (right) and without (left) electric field. The collection efficiency of tungsten particles with the applied voltage of $\pm 7 \text{ kV}$ is about 77% in the present test.

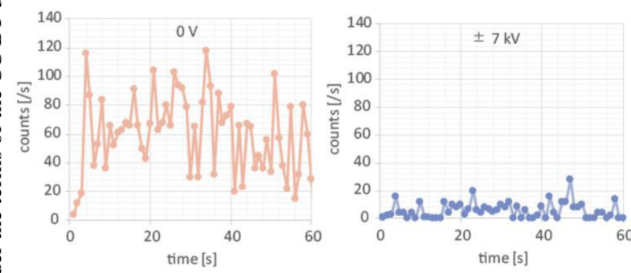


Figure 9: The particle counts ($> 0.3 \mu\text{m}$) when the ceramic block was scraped above the EPS in vacuum with (right) and without (left) electric field.

probe micro analyser to know the composition. The results indicate the main component of silver particles found widely in the bending magnet chambers and ducts were stainless steel and golden particles found in diagnostic chambers were brass.

We cleaned all components in the HEBT by alcohol wiping, air blowing and vacuuming as shown in Fig. 11. Three

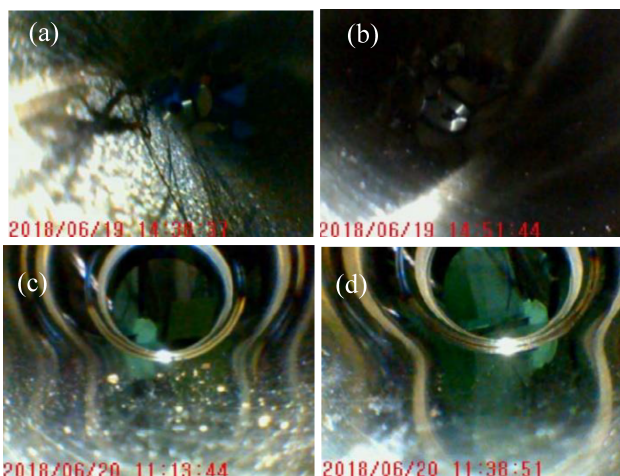


Figure 10: Silver particles (stainless steel) found in a bending magnet chamber. They were removed by wiping (b). Golden particles (brass) found in a diagnostic chamber (c). They are also removed by the wiping (d).

bending magnet chambers were difficult to remove the particles effectively by the wiping procedure because of the complex internal shape. One chamber was renewed and two chambers were rinsed with pressurized ultra-pure water as shown in Fig. 11(e)(f).



Figure 11: Pictures of cleanings of ducts and chambers in the HEBT; alcohol wiping (a,b), air blowing (c), and vacuuming (d). Two bending magnet chambers were rinsed with pressurized ultra-pure water (e,f).

SUMMARY

The NEG-based 3-stage DPS with a compact electrostatic particle suppressor has been developed and the performance

is tested in offline. We demonstrated successfully pressure reduction from 10^{-5} Pa to 10^{-8} Pa both for N₂ and H₂ within the length of 75 cm. After some minor modifications of the system and final cleanings and assembling, the pair DPS will be installed at the both side of the SRILAC in September 2019.

ACKNOWLEDGEMENT

The authors are grateful to Mr. H. Sakurai and Dr. E. MacCallini for technical advice for NEG pumps. The authors are also grateful to Dr. H. Sakai at KEK for useful advice to make the particle counting system in vacuum.

REFERENCES

- [1] M. Odera *et al.*, *Nucl. Instr. Meth. A*, vol. 227, pp. 187, 1984.
- [2] N. Sakamoto *et al.*, “Construction Status of the Superconducting Linac at RIKEN RIBF”, in *Proc. LINAC’18*, Beijing, China, Sep. 2018, pp. 620–625. doi:10.18429/JACoW-LINAC2018-WE2A03
- [3] N. Sakamoto *et al.*, “Development of Superconducting Quarter-Wave Resonator and Cryomodule for Low-Beta Ion Accelerators at RIKEN Radioactive Isotope Beam Factory”, presented at the SRF’19, Dresden, Germany, Jun.-Jul. 2019, paper WETEB1, this conference.
- [4] K. Yamada *et al.*, “Construction of Superconducting Linac Booster for Heavy-Ion Linac at RIKEN Nishina Center”, presented at the SRF’19, Dresden, Germany, Jun.-Jul. 2019, paper TUP037, this conference.
- [5] K. Suda *et al.*, “Fabrication and Performance of Superconducting Quarter-Wavelength Resonators for SRILAC”, presented at the SRF’19, Dresden, Germany, Jun.-Jul. 2019, paper MOP055, this conference.
- [6] O. Kamigaito, K. Ozeki, N. Sakamoto, K. Suda, and K. Yamada, “Measurement of Mechanical Vibration of SRILAC Cavities”, presented at the SRF’19, Dresden, Germany, Jun.-Jul. 2019, paper TUP042, this conference.
- [7] T. Nagatomo *et al.*, “New 28-GHz Superconducting ECR Ion Source for Synthesizing New Super Heavy Elements of Z>118”, in *Proc. ECRIS’18*, Catania, Italy, Sep. 2018, pp. 53–57. doi:10.18429/JACoW-ECRIS2018-TUA3
- [8] K. Morita *et al.*, *JPSJ*, vol. 73, p. 2593, 2004.
- [9] Y. Yano, *Nucl. Instr. Meth. B*, vol. 261, pp. 1009, 2007.
- [10] T. Porcelli, E. MacCallini, P. Manini, M. Mura, and M.F. Urbano, “Experimental Methods for the Assessment of NEG Pumps Working in Dust-Sensitive Environments”, in *Proc. IPAC’18*, Vancouver, Canada, Apr.-May 2018, pp. 3828–3830. doi:10.18429/JACoW-IPAC2018-THPAL076
- [11] Molflow+, <http://molflow.web.cern.ch/>